

# Synthesis of Biodegradable and Antimicrobial Nanogels Based on Carboxymethyl Cellulose

Riham R. Mohamed<sup>1</sup>, Marie E. Fahim<sup>2</sup>, Magdy W. Sabaa<sup>3</sup>

<sup>1</sup>Prof. In Polymer Science and Technology Department of Chemistry, Faculty of Science, Cairo University, Giza-Cairo

<sup>2</sup>B.Sc. Chemistry 2008, Master Student, Department of Chemistry, Faculty of Science, Cairo University, Giza-Cairo

<sup>3</sup>Dr. Prof. in Polymer Science And Technology Department of Chemistry, Faculty of Science, Cairo University, Giza-Cairo

**Abstract**— Nanocomposites based on carboxymethyl cellulose (CMC) and poly (vinyl alcohol) (PVA) were synthesized and characterized via different analysis tools like; FTIR, XRD, TGA, SEM and TEM. These nanocomposites were investigated for different applications like: metal ions uptake, dye uptake, swelling in different pH values and biodegradation in soil. Results showed that as CMC content increased in the CMC/PVA nanocomposites, their swelling increased due to the high hydrophilic nature of CMC. Swelling in pH 9 was maximum for all samples as CMC has acidic character and PVA has a weak acidic nature too. CMC/PVA (2:1) nanocomposites adsorbed much more dyes than the other ratios; this was due to the hydrophilic nature of CMC as compared with PVA. As PVA was introduced in the nano-composites, metal ions adsorption increased, due to the introduction of more chelating centers.

The antimicrobial activity of the nanocomposites was increased as PVA was introduced to give the highest value for antimicrobial activity at the ratio CMC/PVA (1:2), while the biodegradation decreased with the decrease in CMC ratio in the nanocomposites due to the biodegradation nature of CMC.

**Keywords**—Nanocomposites; Carboxymethyl Cellulose; Antimicrobial activity; Dye uptake; metal ions uptake; Biodegradation.

## I. INTRODUCTION

Cellulose is the most abundant naturally occurring polymer, found as the main constituent of plants and natural fibers, such as cotton and linen [1-4]. Chemical modification of cellulose, usually involving esterification or etherification of the hydroxyl groups, has been performed to produce cellulose derivatives, named cellulose derivatives, which are more easily processable and find large applications in the industry [5-8]. Cellulose and its derivatives are environmentally friendly, as they are degradable by several bacteria and fungi present in air, water and soil. Even though, cellulose has not been reached its potential application in many areas because of its infusibility and insolubility.

Great steps have been taken by researchers towards obtaining novel hydrogels based on synthetic, natural or hybrid polymers, which possessed a given swelling properties and/or biocompatibility and bioactivity [9-12]. For many of the above mentioned applications, the biodegradation of the hydrogel is a preferred or a required design variable to be addressed. Indeed a biodegradable hydrogel is neither environmentally friendly nor totally biocompatible in the long term. In the present work, carboxymethyl cellulose (CMC) / poly(vinyl alcohol) nanocomposites were developed and examined for different applications including; heavy metal ions uptake dye uptake and antimicrobial activity. Swelling in different pH values and biodegradation in soil were also tested.

## II. EXPERIMENTAL

### Materials

The pure form of CMC was purchased from Daicel Co. Ltd. Japan (Mol. Wt. 100,000), while PVA was purchased from LOBA Chemie (Mol. Wt. 77,000). N, N,- methylene bis-acrylamide (MBA) was purchased from sigma Aldrich and potassium persulphate (KPS) was purchased from LOBA Chemie, N,N, N'N'- tetramethyl ethylene diamine (TEMED) was purchased from Oxford, Congo Red and Maxilon Blue dyes were purchased from GT, Gurr, London. Cobalt, Nickel and Copper chlorides were purchased from Sigma Aldrich

### Nanocomposites preparation

PVA (1g) was dissolved in 85 ml of water at 45°C, the solution was left to cool at room temperature. 15 ml of acetone was added dropwisely and stirred vigorously with PVA water solution. The solution was cooled at 5°C for 24 hours. Different amounts of CMC were added to the solution with stirring for 30 min. 4.0 mmol MBA, 0.4 mmol KPS and 0.67 mmol TEMED were added into the solution with stirring overnight to carry out polymerization. The solution was poured into a Petri dish and left to dry.

### III. CHARACTERIZATION

#### *Instrumentation*

FTIR spectra were recorded using KBr discs on Testcan Shimadzu IR-Spectrometer (FTIR model 8000) at room temperature within the wave number range of 4000 - 400  $\text{cm}^{-1}$ .

XRD measurements of the powder samples were performed with a PAN analytical X'Pert Powder. The scanning rate was  $1.2^\circ/\text{min}$  and the scanning scope of  $2\theta$  was 5–95 $^\circ$ .

The dry sample, spread on a double sided conducting adhesive tape, pasted on a metallic stub, was coated (100  $\mu$ ) with gold in an ion sputter coating unit (JEOL S150A) for 2 min. and observed in a JEOL-JXA-840A Electron probe microanalyzer at 20 KV.

Atomic absorption was done on A Analyst 100 win lab-Perkin Elmer to determine the amount of metal ions remaining in the hydrogel liquor.

Micrographs of the colloidal nanocomposites were taken using JEM-100S Transmission Electron Microscope (TEM, Japan). The TEM sample was prepared by mixing one dilute drop of prepared aqueous particles dispersed in 5 mL acetone to become slightly turbid solution onto the copper grid and allowing it to dry well. The images of representative areas were captured at suitable magnifications which clarify the morphology and the size of the nanoparticles.

Colorimetric Spectrophotometry was done on Unico 1200 Spectrophotometer at  $\lambda_{\text{max}}$  480 nm for Congo red dye and  $\lambda_{\text{max}}$  580 nm for Maxilon blue dye.

Thermal analysis was done on TGA-50H Shimadzu thermogravimetric analyzer. Samples were heated from 0 - 500 $^\circ\text{C}$  in a platinum pan at a heating rate 10  $^\circ\text{C}/\text{min}$ , under  $\text{N}_2$  atmosphere at a flow rate of 25 mL / min.

Scanning Electron Microscopic (SEM) images were obtained using JEOL (JSM-5200). Samples were prepared by placing a small part of film on a carbon tape on a stub, which was coated with a thin layer of gold.

#### *Antimicrobial measurements*

The antimicrobial activity of CMC, CMC/PVA hydrogels were evaluated against *Staphylococcus aureus* (RCMB 010028), *Streptococcus pneumoniae* (RCMB 010017) and *Bacillus subtilis* (RCMB 010065) as examples of Gram-positive bacteria and *Pseudomonas aeruginosa* (RCMB 010046), *Klebsiella pneumoniae* (RCMB 0010097) and *Escherichia coli* (RCMB 010058) as examples of Gram-negative bacteria and *Aspergillus fumigatus* (RCMB 02569), *Candida albicans* (RCMB 05038) and *Syncephalastrum racemosum* (RCMB 005004) as examples of fungi.

The disks of Whatman filter paper were prepared with standard size (50 mm diameter) and kept into 10 screw capped wide mouthed containers for sterilization. These bottles were kept into hot air oven at temperature 150  $^\circ\text{C}$ , then the sterilized filter paper disks impregnated with a solution of the test compound in DMSO (1 mg/ml) were placed on nutrient agar plate seeded with the appropriate test organism in triplicates. Standard conditions of 106 CFU/mL (colony forming U/mL) and 104 CFU/mL were used for antibacterial and antifungal assay, respectively. Petri dishes (9 cm in diameter) were used and the disks of filter paper were inoculated in each plate. Ampicillin, Gentamicin and Amphotericin B were used as reference drugs against Gram-positive bacteria, Gram-negative bacteria and fungi, respectively. DMSO alone was used as control at the same abovementioned concentration and during this, there was no visible change in bacterial growth. The plates were incubated at 37  $^\circ\text{C}$  for 24 h for bacteria and 48 h at 25 $^\circ\text{C}$  for fungi. After incubation, antimicrobial activity was evaluated by measuring the inhibition zones against the test organisms and was compared with that of the standard. Antimicrobial activity was expressed as inhibition diameter zones in millimeters (mm). The experiments were carried out in triplicates, the average zone of inhibition was calculated and the data was expressed as mean ( $\pm$ standard deviation) (SD)

#### IV. APPLICATIONS DONE ON CMC/PVA HYDROGELS SWELLING STUDIES

Water uptake of hydrogels was studied at 30°C in doubly distilled water and in buffered solutions of different pH values; 4 and 9. A known weight of pre-dried sample was placed into a flask with 25 mL water or buffer solution of the given pH and kept undisturbed in a thermostated water bath (at 30°C) until equilibrium swelling was reached (~ 72 hours). After wiping off the excessive water on the sample surface with filter paper, the weight of the swollen samples was measured. The swelling percentage was determined according to the following equation:

$$\text{Water uptake \%} = [(W_s - W_o) / W_o] \times 100$$

Where;

$W_s$  = weight of wet sample.

$W_o$  = weight of dry sample.

The results obtained represent the average of three comparable experiments for each sample.

#### *Dye uptake*

The dye uptake of CMC and CMC/PVA hydrogels were measured. Two types of dyes were used; Congo red (acidic dye) and Maxilon Blue (cationic dye). Different known concentrations of the dye were prepared. 25 mL of the dye solution of a known concentration was added to 100 mg of the hydrogel in 100 mL flat bottomed flask and stirred continuously at room temperature for 24 h to reach equilibrium. After filtration, the concentration of the dye in the filtrate was determined colorimetrically at wavelength; 480 nm and 580 nm for the investigated dyes, respectively.

The variation of dye adsorption by CMC and CMC/PVA nanocomposites was determined by a graph relation between the quantity of the adsorbed dye and the dye concentration equivalent.

The quantity of the adsorbed dye was calculated according to the following equation [13]:

$$Q = (N_a - N_s) / W$$

Where;

$Q$  = fixed quantity of dye (mg) / hydrogel (g).

$N_a$  = Quantity of original dye (mg).

$N_s$  = Quantity of remaining dye after adsorption (mg).

$W$  = mass of hydrogel (g)

And the dye concentration equivalent was calculated by the following equation:

$$C_0 = \epsilon \times C_{eq}$$

Where;

$C_0$  = The concentration of remaining dye after adsorption. (mg/L)

$C_{eq}$  = The dye concentration equivalent. (mg/L)

$\epsilon$  = slope at maximum wavelength (mg/L)<sup>-1</sup>

#### *Adsorption of heavy metal ions*

Chloride salts of the heavy metal ions ( $Co^{2+}$ ,  $Ni^{2+}$  and  $Cu^{2+}$ ) solutions of known concentrations were prepared (0.05 mol/L), then 0.1g of the hydrogel was soaked into 25 mL salt solution, stirred for 24 h at room temperature till equilibrium was attained. After filtration, the remained metal ions in the solution were estimated using atomic absorption technique - after soaking the hydrogel- to determine the amount of metal ions remained in the liquor and consequently, the amount of adsorbed metal ions could be calculated by difference and also metal ion retention (retention capacity) according to the following relations:

$$q \text{ (mg/g wet weight)} = V (C_o - C_A) / 1000 W$$

Where;

$V$  (L) is the volume of the salt solution,  $W$  (g) is the weight of the hydrogel,  $C_o$  (mg/L) is the initial metal concentration and  $C_A$  (mg/L) is the metal concentration at definite time.

Retention capacity (ppm/g) = Conc. of adsorbed metal ions in polymer (ppm) / Weight of dry polymer (g)

#### *Biodegradation in soil*

0.1g of the hydrogels were taken and buried in soil under the same conditions. Irrigation was done once a week "before samples were buried to avoid their swelling". Samples were taken out every week, clean them well from any soil particles and reweigh them. The last two steps were repeated for 4 weeks.

The weight loss was determined using the following equation:

$$\text{Weight loss} = (W_1 - W_2 / W_1) \times 100$$

Where;  $W_1$  is the initial weight of sample and  $W_2$  is the weight of sample after burial

## V. RESULTS AND DISCUSSION

### *Characterization of CMC/PVA nanocomposites*

FTIR spectrum of CMC -Fig (1) - showed a specific peak at 1412 cm<sup>-1</sup> which could be assigned to the symmetrical COO - group stretching vibration, asymmetrical stretching vibration of the COO- group near 1550 cm<sup>-1</sup> and 1100 cm<sup>-1</sup> characteristic for C-OH stretching.

For the FTIR spectrum of PVA, the following peaks were recorded: 2800–3000  $\text{cm}^{-1}$  which corresponds to the stretching of  $-\text{CH}$  groups in alkanes and a wide-strong absorption peak at 3500–3350  $\text{cm}^{-1}$  is associated with the stretching of  $\text{O}-\text{H}$  from the intermolecular and intramolecular hydrogen bonds [14]. Peaks between 1750 and 1735  $\text{cm}^{-1}$  were due to the stretching of  $\text{C}=\text{O}$  and  $\text{C}-\text{O}$  from acetate groups remaining from PVA [15].

As for the prepared nanocomposites, they contain a strong absorption peak at 3400  $\text{cm}^{-1}$  coming from both the stretching of  $\text{O}-\text{H}$  of PVA and also the  $\text{O}-\text{H}$  stretching vibrations of CMC chains. These nanocomposites had a broad peak near 1100  $\text{cm}^{-1}$  characteristic for  $\text{C}-\text{OH}$  stretching coming from PVA, and a strong peak at 1587–1650  $\text{cm}^{-1}$  corresponding to the  $-\text{COOH}$  groups in CMC.

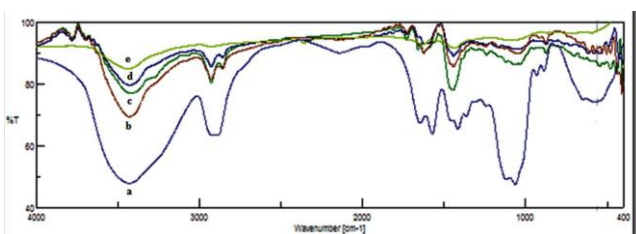


**Fig (1): FTIR for a) CMC , b) CMC:PVA (1:1) , c) CMC:PVA (2:1), d) CMC:PVA (1:2) and e) PVA.**

X-Ray diffraction analysis is represented in Fig (2). The high crystalline structure of PVA was confirmed by the observed intense and strong peaks. The X-Ray diffraction of CMC and CMC/PVA nanocomposites are also given for comparison. The diffraction peak of carboxymethyl cellulose is located around  $21^\circ$  and it is very weak, indicating low crystallinity. However diffraction peaks of pure PVA are located at  $20^\circ$ – $20^\circ$  and  $23^\circ$  which are strong and at  $40^\circ$  which is weak indicating the high crystalline structure of PVA. [16,17] The X-ray investigations showed that CMC/PVA nanocomposite (1:2) with higher concentration of PVA contained two diffraction strong peaks, at  $20^\circ$ – $20^\circ$  and  $23^\circ$  and other weak one occurring at  $40^\circ$ . On the other hand nanocomposites with lower PVA concentration showed a weaker peak at  $20^\circ$ – $23^\circ$ . The weak diffraction peak of CMC in the nanocomposites at  $20^\circ$ – $21^\circ$  was merged with that of the strong peak of PVA at  $20^\circ$ – $20^\circ$ .

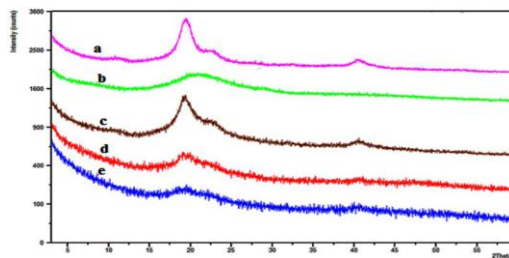


**Fig (2): X-Ray Diffraction for a) PVA, b) CMC, c) CMC: PVA (1:2), d) CMC: PVA (2:1) and e) CMC:PVA (1:1).**

The thermogravimetric analysis (TGA) of CMC, PVA and their nanocomposites is represented in Table (1). PVA was thermally stable till  $280^\circ\text{C}$ , then it started to degrade as it lost almost 75% of its weight at  $400^\circ\text{C}$  and more than 80% at  $500^\circ\text{C}$ , while CMC was thermally stable till  $240^\circ\text{C}$  then started to degrade and lost 65% of its weight at  $400^\circ\text{C}$  and lost more than 70% at  $500^\circ\text{C}$ . The weight loss of CMC before  $240^\circ\text{C}$  is due to the loss of water molecules. The relatively low IDT of the parent CMC is mainly attributed to the presence of  $\text{COOH}$  group which may decompose to the  $\text{CO}_2$  gas. The same behavior was reported by Biswal and Singh for CMC [18]. All nanocomposites were almost thermally stable till around  $240$ – $250^\circ\text{C}$ . The IDT of CMC/PVA (1:1) was  $250^\circ\text{C}$ .

At  $400^\circ\text{C}$ , it lost 70% of its weight and lost 80% at  $500^\circ\text{C}$ . Nanocomposites CMC/PVA (2:1) was the most stable one due to its higher CMC content as it lost 65% of its weight at  $400^\circ\text{C}$ . Nanocomposites CMC/PVA (1:2) was the least stable one as it lost 75% of its weight as  $400^\circ\text{C}$ .

**Table 1**  
**TGA for CMC, PVA and CMC/PVA nanogels**

Sample	IDT ( $^\circ\text{C}$ )	350 $^\circ\text{C}$	400 $^\circ\text{C}$	450 $^\circ\text{C}$	500 $^\circ\text{C}$
<b>Weight loss %</b>					
CMC	240	62	65	70	72
PVA	280	65	75	80	83
CMC:PVA (2:1)	245	60	65	70	80
CMC:PVA (1:1)	250	68	70	76	80
CMC:PVA (1:2)	270	68	75	80	85

Fig. (3) (a, b and c) showed the TEM images of CMC/PVA nanocomposites with different CMC concentrations in the 1% PVA acetone/water solution namely: (a) 1:1, (b) 1:2, and (c) 2:1. It is found that the morphology of the nanocomposites is greatly affected by the initial CMC concentration in the solution. In Fig. 3 (a), the CMC/PVA nanocomposites (1:1) showed sphere-shaped particles with a diameter varying between 4.5-20 nm. Figure 3(b) with lower concentration of CMC (1:2) resulted in nanogels with bigger diameters of 20-40 nm so a lower picture magnification was needed to enhance the figure quality. The increase in CMC concentration (2:1) resulted in a decrease in CMC/PVA nanocomposites size as shown in Fig. 3 (c) with a diameter varying between 3-5 nm.

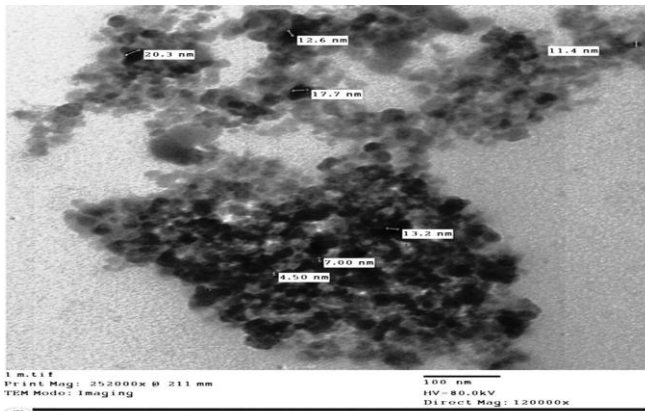


Fig (3 a)

Fig (3a): TEM image for CMC: PVA (1:1).

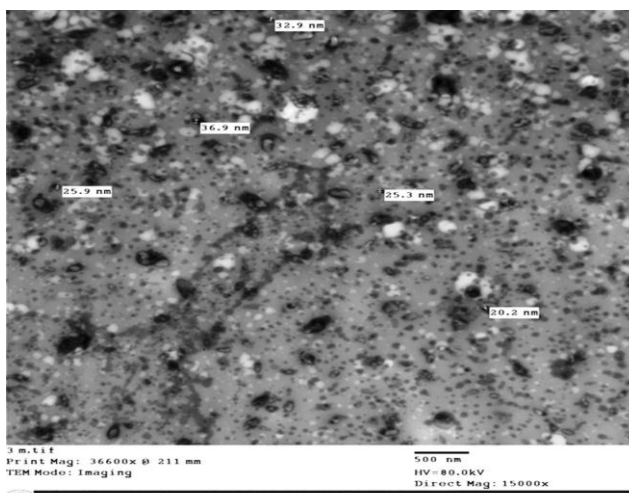


Fig (3 b)

Fig (3b) TEM image for CMC: PVA (1:2).

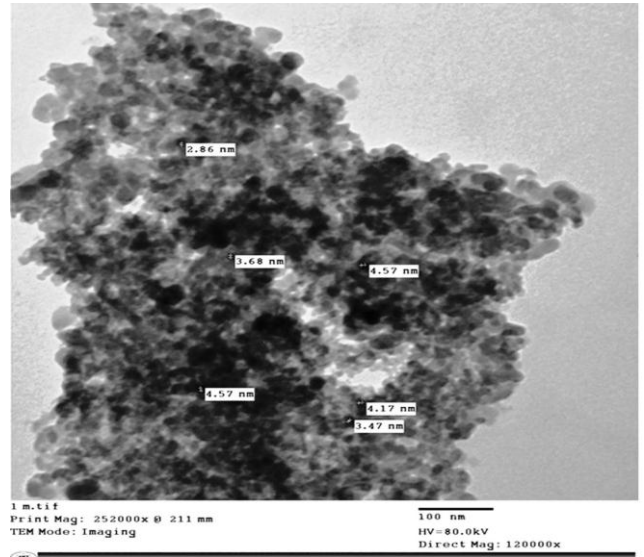


Fig (3c)

Fig (3c) TEM image for CMC: PVA (2:1).

SEM images of CMC, PVA and their nanocomposites of different compositions are illustrated in Fig. (4). The morphology transition of nanocomposites from highly lumpy-form surface- due to the presence of bulky -COOH groups in CMC as shown in Fig. 4 (a) to a more fibrous structure when PVA was introduced into the nanocomposites. As the concentration of CMC increased in the nanocomposites, the lumpy-form-surface overcame the fibrous structure as shown in Fig. 4 (d). The CMC/PVA (1:2) nano-composites showed the fibrous nature of PVA due to its high content as shown in Fig 4 (c).

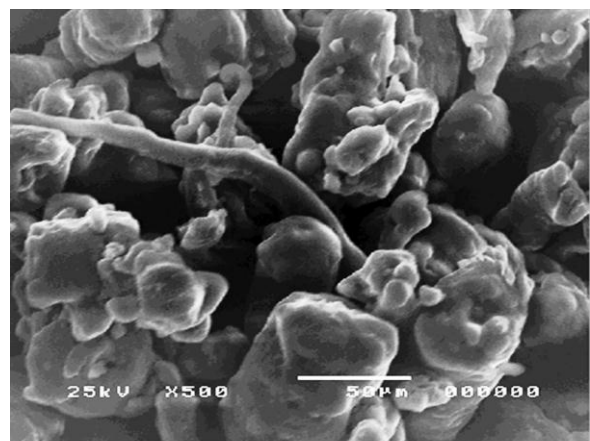
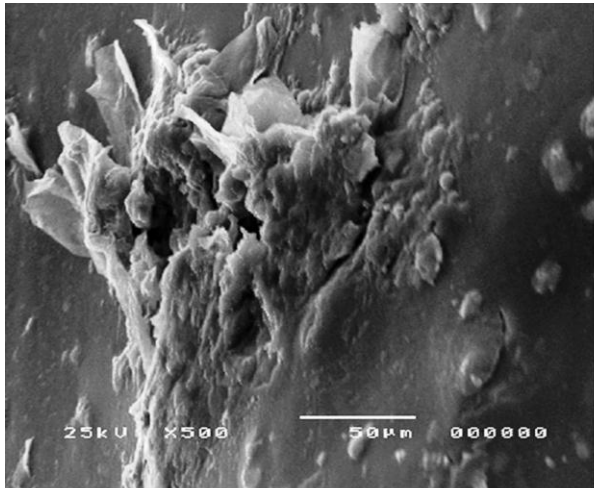
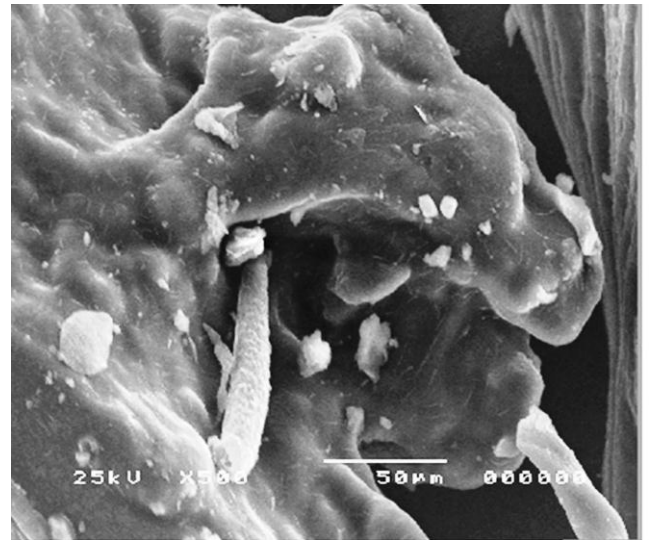


Fig (4 a)

Fig (4a): SEM image for CMC.



**Fig (4 b)**  
**Fig 4(b): SEM image for CMC: PVA (1:1)**



**Fig (4d)**

**Fig 4 (d) SEM image for CMC: PVA (2:1)**

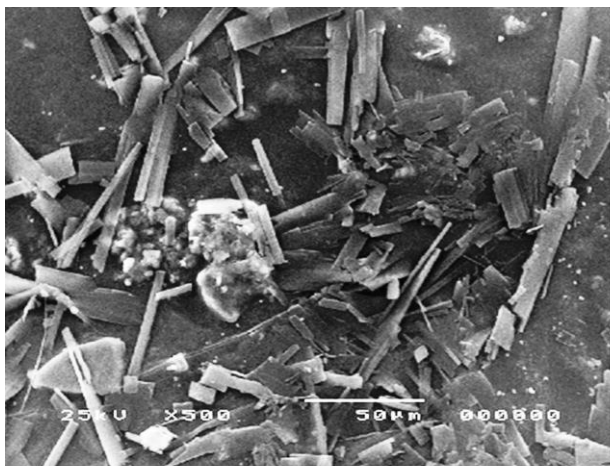


**Fig (4c)**  
**Fig 4 (c) SEM image for CMC: PVA (1:2)**

The swelling behavior of the investigated nanocomposites in different pH values is shown in Table (2). The results indicated that for all pH values, CMC exhibited the highest swelling ratio (%), whereas, PVA exhibited the least swelling ratio. As CMC content increases in CMC/PVA nanocomposites, their swelling ability increases due to the high hydrophilicity of CMC. Swelling at pH 9 is maximum for all samples as CMC has acidic character and PVA has a weak acidic nature too, while the swelling is minimum at acidic pH (4) and it is intermediate in the neutral pH (7)

**Table (2):**  
**Swelling ratio of CMC, PVA, CMC/PVA nanogels in different ratios**

pH	Sample	Swelling %
4	PVA	123±1
	(CMC:PVA) (1:2)	679±2
	(CMC:PVA) (1:1)	731±2
	(CMC:PVA) (2:1)	871±3
	CMC	992±3
7	PVA	158±1
	(CMC:PVA) (1:2)	776±2
	(CMC:PVA) (1:1)	817±2
	(CMC:PVA) (2:1)	970±2
	CMC	1059±3
9	PVA	212±1
	(CMC:PVA) (1:2)	818±2
	(CMC:PVA) (1:1)	910±3
	(CMC:PVA) (2:1)	1010±3
	CMC	1168±2

*Applications of CMC nanocomposites:*

CMC/PVA (2:1) nanocomposites adsorb much more Congo red dye than the other nanocomposites, followed by CMC/ PVA (1:1), CMC and CMC/PVA (1:2), Fig (5) a. This is mostly attributed to the more hydrophilic nature of CMC as compared with PVA. The same attitude was observed for Maxilon blue dye, but with much higher adsorption capacity for the dye due to the basic character for this dye and the acidic nature for the CMC/PVA nanocomposites. Fig (5) b.

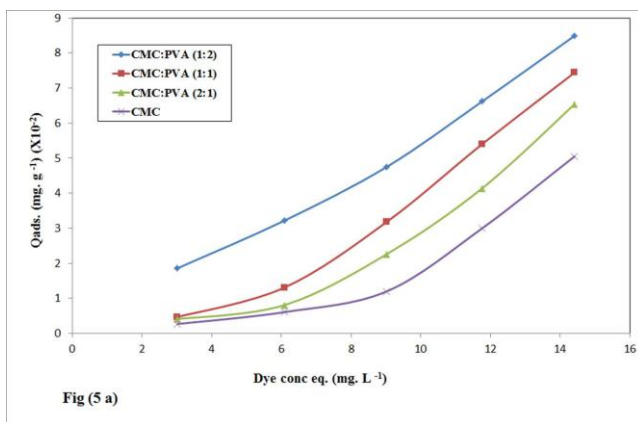


**Fig (5 a): Congo Red dye uptake by CMC and CMC: PVA nanogels.**

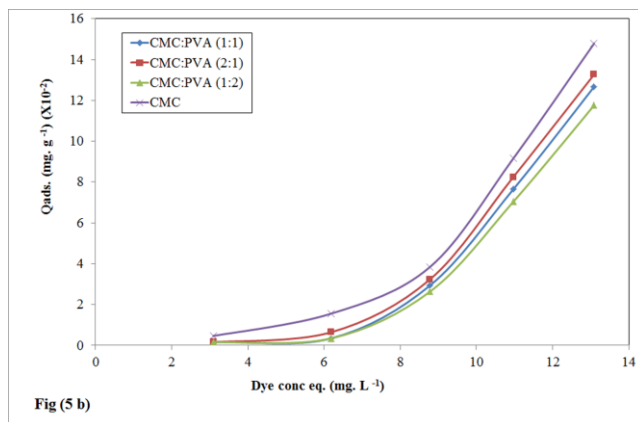


**Fig (5 b): Maxilon Blue dye uptake by CMC and CMC: PVA nanogels.**

CMC has two chelating groups –OH, –COOH so it can adsorb metal ions, as PVA was introduced into the nanocomposites, metal ions adsorption increased, due to the introduction of more chelating centers in the nanocomposites.

CMC: PVA (1:2) adsorbed metal ions the most among the other ratios due to the higher content of PVA. As

**Table (3):  
Concentration of adsorbed metal ions (ppm) and retention capacity (ppm/g) of CMC, CMC/PVA nanogels**

Sample	Cu <sup>2+</sup>		Co <sup>2+</sup>		Ni <sup>2+</sup>	
	Metal ion uptake (ppm)	Retention capacity (ppm/g)	Metal ion uptake (ppm)	Retention capacity (ppm/g)	Metal ion uptake (ppm)	Retention capacity (ppm/g)
CMC	648	2160	424	1413	370	1233
CMC: PVA (1:1)	762	2540	477	1590	440	1467
CMC: PVA (1:2)	762	2540	513	1710	440	1467
CMC: PVA (2:1)	667	2223	424	1413	405	1350

shown -in Table (3) - the selectivity of nanocomposites towards metal ions was in the following order:



These obtained results coincide well with other results reported in the literature [19].

**Table 4:**  
Antimicrobial activity of CMC/PVA nanogels towards different types of bacteria and fungi

Sample Tested microorganisms	PVA :CMC 1:1	CMC	PVA :CMC 1:2	PVA :CMC 2:1	Standard
<b>FUNGI</b>					<i>Amphotericin B</i>
<i>Aspergillus fumigatus</i> (RCMB 02569)	17.8 ± 0.63	12.6 ± 0.58	15.6± 0.44	20.3± 0.25	23.7± 0.10
<i>Candida albicans</i> (RCMB 05038)	NA	NA	NA	NA	21.9± 0.12
<i>Syncephalastrum racemosum</i> (RCMB 005004)	15.8 ± 0.58	10.2 ± 0.44	13.3± 1.2	17.4± 0.37	20.3± 0.12
<b>Gram Positive Bacteria:</b>					<i>Ampicillin</i>
<i>Staphylococcus aureus</i> (RCMB 010028)	17.4 ± 0.44	13.2 ± 0.44	15.4± 0.58	19.2± 0.63	28.9± 0.14
<i>Streptococcus pneumoniae</i> (RCMB 010017)	18.2± 0.63	14.6 ± 0.43	16.9 ± 0.44	20.1 ± 0.58	25.3± 0.58
<i>Bacillus subtilis</i> (RCMB 010065)	19.3± 0.58	16.2± 0.53	17.2± 0.25	20.9±0.67	26.4± 0.34
<b>Gram negative Bacteria:</b>					<i>Gentamicin</i>
<i>Pseudomonas aeruginosa</i> (RCMB 010046)	NA	NA	NA	NA	26.3± 0.15
<i>Klebsiella pneumoniae</i> (RCMB 0010097)	19.3 ± 0.44	14.6 ± 0.58	16.4± 0.44	21.2 ±0.58	17.3± 0.12
<i>Escherichia coli</i> (RCMB 010058)	16.9 ± 0.58	13.7 ± 1.2	13.9± 0.63	18.1 ±0.46	27.3± 0.44

As a general phenomenon, CMC showed the lowest antimicrobial activity compared with the three ratios of nanocomposites. The antimicrobial activity of nanocomposites increased with the increase of PVA concentration to give the highest value at the ratio CMC/PVA (1:2), Table (4). An acceptable mechanism elucidating the antimicrobial activity of CMC/PVA has been postulated in literature. The chelating of metals, suppression of spore elements and binding to essential nutrients to microbial growth [20].

It is established that the chelating groups of CMC/PVA (1:2) nanocomposites have excellent metal-binding capacity which explains their better antibacterial activities [21].

For the Gram +ve bacteria, the highest value for the ratio CMC/PVA (1:2) was in case of *Bacillus subtilis* (RCMB 010065) and *Aspergillus fumigatus* (RCMB 02569) as a fungi.

CMC/PVA nanocomposites showed higher antibacterial activity against the Gram positive bacteria *Staphylococcus aureus* (RCMB 010028), *Streptococcus pneumoniae* (RCMB 010017) and *Bacillus subtilis* (RCMB 010065) than Gram negative bacteria *Escherichia coli* (RCMB 010058). This may be attributed to their different cell walls. The cell wall of Gram positive bacteria is fully composed of peptide poly glycogen. The peptidoglycan layer is composed of networks with plenty of pores, which allow foreign molecules to come into the cell without difficulty and allows more rapid absorption of ions into the cell. The cell wall of Gram negative bacteria is made up of a thin membrane of peptide poly glycogen and an outer membrane constituted of lipopolysaccharide, lipoprotein and phospholipids. Because of the complicated bilayer cell structure, the outer membrane is a potential barrier against foreign molecules with high molecular weight.

In case of Gram –ve bacteria, *Klebsiella pneumoniae* (RCMB 0010097), CMC/PVA nanocomposites in all ratios gave even higher antibacterial activity than the control antibiotic itself (Gentamicin).

Compared to other polymers, PVA biodegradation was much slower in the same soil environments (Chiellini et al., 2000). A detailed investigation was carried out on PVA sheets buried in 18 different natural soil sites, with different compositions and climate conditions. However, after two years of incubation only very limited weight losses (less than 10%) were recorded under natural weathering conditions (Sawada, 1994; Chen et al., 1997). Table (5) shows that CMC degraded so easily in soil as it lost a lot of its weight upon burial; CMC lost about 64% of its weight at the fourth week of burial. As PVA was introduced into the nanocomposites, biodegradation process decreased with the increase in the content of PVA in the nanocomposites. These results are in agreement with PVA biodegradation data in literature [22].

## VI. CONCLUSION

Nanocomposites composed of carboxymethyl cellulose (CMC) and poly (vinyl alcohol) (PVA) were synthesized and characterized by different analysis tools including; FTIR, XRD, TGA, SEM and TEM.

The obtained results showed that:

As CMC content increased in the CMC/PVA nanocomposites, their swelling ability increased due to the high hydrophilicity of CMC. Swelling at pH 9 was maximum for all samples as CMC has acidic character and PVA has a weak acidic nature too.

CMC/PVA (2:1) nanocomposites adsorbed much more dye than the other ratios; this was due to the hydrophilic nature of CMC as compared with PVA. As PVA was introduced in the nanocomposites, metal ions adsorption increased, due to the introduction of more chelating centers.

The antimicrobial activity of the nanocomposites increased with the introduction of PVA to give the highest value for antimicrobial activity at the ratio CMC/PVA (1:2).

As PVA content increased in the nanocomposites, biodegradation decreased due to the fact that the increase in the concentration of PVA came on the expense of CMC. The latter is known for its biodegradation as being a derivative of a natural polymer.

## REFERENCES

- [1] P. R. Salgado, V. C. Schmidt, S. E. Molina Ortiz, A. N. Mauri, and J. B. Laurindo (2008) Biodegradable foams based on cassava starch, sunflower proteins and cellulose fibers obtained by a baking process, *Journal of Food Engineering*, 85 (3); 435–443.
- [2] W. Liu, M. Misra, P. Askel, L.T. Drzal, A.K. Mohanty (2005) Green composites from soy based plastic and pineapple leaf fiber: fabrication and properties evaluation, *Polymer*, 46 (8); 2710–2721.
- [3] K.G. Satyanarayana, G.G.C. Arizaga, F. Wypych (2009) Biodegradable composites based on lignocellulosic fibers—an overview, *Progress in Polymer Science*, 34 (9); 982–1021.
- [4] R. L. Wu, X. L. Wang, F. Li, H. Z. Li, Y. Z. Wang (2009) Green composite films prepared from cellulose, starch and lignin in room-temperature ionic liquid, *Bioresource Technology*, 100(9); 2569–2574.
- [5] S. Boufi, M. N. Belgacem (2006) Modified cellulose fibres for adsorption of dissolved organic solutes, *Cellulose*, 13(1); 81–94.
- [6] J. Zhang, N. Jiang, Z. Dang, T. J. Elder, A. J. Ragauskas (2008) Oxidation and sulfonation of celluloses, *Cellulose* 15 (3) 489–496.
- [7] Y. Kitkulnumchai, A. Ajavakom, M. Sukwattanasinitt (2008) Treatment of oxidized cellulose fabric with chitosan and its surface activity towards anionic reactive dyes, *Cellulose*, 15(4); 599–608.
- [8] D. Pasquini, E. Teixeira, A. A. Curvelo, M. N. Belgacem, A. Dufresne (2008) Surface esterification of cellulose fibres: processing and characterisation of low-density polyethylene/cellulose fibres composites, *Composites Science and Technology*, 68 (1); 193–201.
- [9] D.R. Chambers, H.H. Fowler, Y. Fujiura, F. Masuda (1992) Super-absorbent polymer having improved absorbency properties. US Patent 5145906.
- [10] M.J. Smith, T.H. Flowers, M.J. Cowling, H.J. Duncan (2003) Release studies of benzalkonium chloride from hydrogel in a freshwater environment. *Journal of Environmental Monitoring* 5 (2); 359–362.
- [11] M.S. Johnson, The effects of gel-forming polyacrylamides on moisture storage in sandy soils (1984). *Journal of Science and Food Agriculture*, 35 (11); 1063–1066.
- [12] M. Bakass, A. Mokhlisse, M. Lallemand (2002) Absorption and desorption of liquid water by a super-absorbent polymer: effect of polymer in the drying of the soil and the quality of certain plants. *Journal of Applied Polymer Science*, 83 (2); 234–243.
- [13] G. Crinia, F. Gimberta, C. Roberta, B. Martelb, O. Adama, N. Morin-Crinia, F. De Giorgia, P. Badot (2008). The removal of Basic Blue 3 from aqueous solutions by chitosan-based adsorbent: Batch studies. *Journal of Hazardous Materials*, 153; 96–106.
- [14] A.S. Gilbert (1999) Hydrogen Bonding and Other Physicochemical Interactions Studied By IR and Raman Spectroscopy. *Encyclopedia of Spectroscopy and Spectrometry*; 837–843.
- [15] H.S. Costa, A.A.P. Mansur, E.F. Barbosa-Stancioli, M.M. Pereira, H.S. Mansur (2008) Morphological, mechanical and biocompatibility characterization of macroporous alumina scaffolds coated with calcium phosphate/PVA. *Journal of Material Science*, 43; 510–524.
- [16] Noorhanim Ahad, Elias Saion, and Elham Gharibshahi, Structural, Thermal, and Electrical Properties of PVA-Sodium Salicylate Solid Composite Polymer Electrolyte, *Journal of Nanomaterials*, Volume 2012, Article ID 857569, 10 July 2012

**International Journal of Emerging Technology and Advanced Engineering**

**Website: [www.ijetae.com](http://www.ijetae.com) (ISSN 2250-2459, ISO 9001:2008 Certified Journal, Volume 7, Issue 5, May 2017)**

- [17] Cheng-Ming Tang 1 , Yi-Hung Tian 1 and Shan-Hui Hsu, Poly(vinyl alcohol) Nanocomposites Reinforced with Bamboo Charcoal Nanoparticles: Mineralization Behavior and Characterization, *Materials* 2015, 8, 4895-4911
- [18] Biswal,D.R.; Singh, R.P. *carbohydr polym* 2004, 57, 379.
- [19] R. Kh. Hyam, R. Arun Raud (2014) Adsorption studies for the removal of heavy metal by chitosan – g- poly( acrylacid-co-acrylamide) composite, *Science Journal of Analytical Chemistry*,2(6);67-70.
- [20] \ C.G. Rejane, D.B. Douglas, B.G.A. Odilio, A Review of the Antimicrobial Activity of Chitosan, *Polímeros, Ciência e Tecnologia* 19 (3) (2009) 241–247.
- [21] R.G. Cuero, G. Osuji, A. Washington, N-methylcarboxy chitosan inhibition of Aflatoxin production; role of zinc, *Biotechnol. Lett.* 13 (1991) 441–444.
- [22] The University of Manchester Faculty of Life Sciences, Fungal Biodegradation Of Polyvinyl Alcohol In Soil And Compostenvironment. A Thesis Submitted to the University of Manchester for the Degree of Doctor of Philosophy In the Faculty of Life Sciences 2013 Somayeh Mollasalehi.